Electric Power Systems Research 229 (2024) 110061

Contents lists available at ScienceDirect

Electric Power Systems Research

journal homepage: www.elsevier.com/locate/epsr

Determining total cost of ownership and peak efficiency index of dynamically rated transformer at the PV-power plant

Wílerson Venceslau Calil [a,b], Kateryna Morozovska [c], Tor Laneryd [a], Eduardo Coelho Marques da Costa [b,*], Maurício Barbosa de Camargo Salles [b]

[a] Hitachi Energy, Västerås, Sweden
[b] Polytechnic School of the University of São Paulo, São Paulo, Brazil
[c] KTH Royal Institute of Technology, Stockholm, Sweden

ARTICLE INFO

Keywords:
Dynamic transformer rating
Power transformers
Smart-grid
Solar power

ABSTRACT

Dynamic rating of the transformer is a promising technology, which is suitable for various applications. Using dynamic rating for connecting renewable energy is believed to be beneficial for the economy and flexibility of the power system. However, to safely deploy such operation strategies, it is important to have more precise estimates for the total costs of owning such units and determine how effective such operation method is for a solar power plant. This study proposes a method for calculating total ownership costs (TOC) of dynamically rated transformers used for the connection of the solar power plant to the grid as well as analyzes its efficiency. The sensitivity analysis looks into the change in TOC and peak efficiency index (PEI) after considering reactive power dispatch. Results of this study also show how TOC, PEI, and load and no-load losses change depending on the transformer size.

1. Introduction

The concept of dynamic rating allows grid operators to safely extend the capacity of power components beyond the nameplate rating. Although, more popular as an operation strategy for overhead lines, dynamic rating of power transformers is currently gaining more attention from the industry [1]. Dynamic transformer rating (DTR) can be defined as the maximum load, which the transformer can sustain under time-varying load and/or environmental conditions [2,3]. Power transformers are usually sized and designed conservatively, to withstand extreme combinations of load and weather conditions, which rarely come together in practice, and the thermal behavior of the transformer insulation is a key factor during the design process [4].

According to previous studies, it is evident that DTR can be safely applied without endangering component life expectancy and/or keeping the increase in loss of life sufficiently low [5]. The usage of the dynamic rating could optimize the characteristics of power transformers to be installed and therefore result in a better project economy and lower need for initial investment [2,3,6,7].

DTR is the method that arises from the traditional thermal modeling of the transformer which takes place during the design and specification process, but in contrast to the power limits being constant, they are changed depending on the real-time weather and loading conditions. Hence, the first studies on DTR are highly focused on the development of thermal models for better assessment of transformer temperature distribution as well as insulation aging under high load conditions [1,2,8–10]. The explorations of the variability of the transformer's thermal behavior have led to case studies on the performance of dynamically rated power transformers in a distribution network [11–14]. There are several studies evaluating the benefits of DTR in the distribution network related to the system's stability [15,16] and available transmission capacity [17]. In [18,19] authors show the benefits of using DTR and determine the maximum allowable loading for a given transformer.

Overload implies risks during power system operation when the load profile exceeds the nameplate rating of some power devices in the system. Reliability and risk analysis of DTR operation in a distribution network are evaluated in [3,6,20]. DTR implementation also brings additional challenges of operation safety and reliability, which is highly dependent on the accuracy of load and capacity forecasting; these issues are addressed using probabilistic risk assessment in [21,22].

DTR applications for renewable energy have been analyzed in a few literature resources, however, often they focus on wind power development [23–25]. The studies of DTR usage for wind power integration focus on case studies and evaluate the share of wind power in the grid after DTR application [23,26,27] as well as potential expansion of wind sites using the same transformer [3,25] or design of future wind farm with DTR in mind and transformer size reduction [6,28,29].

* Correspondence to: Polytechnic School, University of São Paulo, Av. Prof. Luciano Gualberto, 380 - Butantã, São Paulo - SP, 05508-010, Brazil.
E-mail address: educosta@usp.br (Eduardo Coelho Marques da Costa).

https://doi.org/10.1016/j.epsr.2023.110061
Received 1 August 2023; Received in revised form 21 November 2023; Accepted 3 December 2023
Available online 13 January 2024

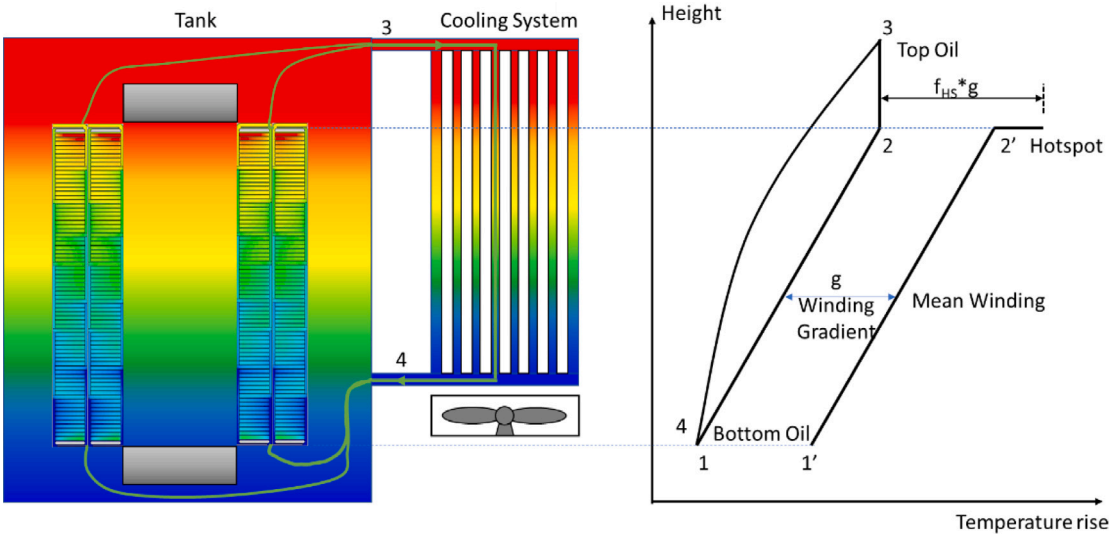

Fig. 1. Temperature map versus tank height.

While the benefits and limitations of DTR applications for wind power have been explored, only a few case studies look into using DTR to improve the utilization of transformers at solar power plants. In [30], DTR is studied in conjunction with high PV penetration in a distribution network; the study has identified that DTR has the potential to increase the share of solar power in the energy mix. Given the limited number of studies on DTR for PV-plant applications, this study aims to perform cost analysis and performance assessment to identify the total ownership costs (TOC) and the peak efficiency index (PEI) for a PV plant with DTR. Power transformers being explored in this study have rated power of 55 to 100 MVA. This approach allows grid operators to test the impact of DTR on the efficiency and costs of transformer operation.

2. Methodology

The methodology uses a data set of optimized selection of solar power transformers. The transformers range from 50 MVA to 175 MVA with a primary voltage of 33 kV to 36 kV and a secondary side voltage of 138 kV to 500 kV. The proposed method uses no-load and load loss capitalization as parameters, which also depend on the most cost-effective electrical steel available on the market. The higher steel quality reduces losses in the transformer, which also leads to higher costs. Therefore, depending on the capitalization factor, it is possible to optimize the transformer's core design finding the right balance between costs and losses. The model needs to be corrected for the loss of life as a function of the transformer's temperature distribution. During colder months the transformer experiences lower loss of life compared to the warmer months given the same load level. Fig. 1 shows the transformer's temperature distribution, where the cooling media flow can be observed. In Fig. 1 points 1 and 1' are the lowest temperature points found in the equipment, also known as Bottom Oil temperature. Since the heat is mainly generated in the core and transformer windings when the oil flows through them the temperature increases progressively from the bottom to the top of the tank, as shown in Fig. 1.

The most critical transformer temperature is found in the transformer windings and is named the hotspot temperature. The hotspot temperature distribution is non-linear and is governed by the hotspot factor, which is a ratio between maximum and average losses in the windings. The mean winding absolute temperature MO_{abs} is determined by parameters such as the top oil temperature TO, bottom oil temperature BO, hotspot temperature HS, hotspot factor f_{HS}, and the ambient temperature T_{amb} as in (1).

$$MO_{abs} = \frac{(TO - BO)}{2} + \frac{(HS - TO)}{f_{HS}} + T_{amb} \tag{1}$$

Overload conditions have more effect on the smaller size transformers and the temperature distribution in windings and insulation, therefore it is necessary to do the temperature correction and take the transformer size into account during the design stage. The temperature correction in the transformer windings requires distinguishing between the types of associated losses. For Ohmic losses PW and winding eddy current losses PE, the correction factor is directly proportional to the temperature, as expressed in (2) [31].

$$f_{PW} = f_{PE} = \frac{(234.5 + T_{\theta})}{(234.5 + T_{ref})} \tag{2}$$

where f_{PW} and f_{PE} are the temperature correction factors for the Ohmic losses and eddy current losses respectively; T_{ref} is the reference temperature defined in the standard which is normally 75 °C for non-thermally upgraded paper and 85 °C for thermally upgraded paper and, T_{θ} is the temperature, which the material is subjected to.

The stray loss PS phenomenon works the opposite way, meaning that the higher the temperature is, the lower the stray losses become. This occurs because of the greater conductivity of metallic parts of the transformer, as shown by (3) [31].

$$f_{PS} = \frac{(234.5 + T_{ref})}{(234.5 + T_{\theta})} \tag{3}$$

where f_{PS} is the temperature correction factor for stray losses.

The load losses LL are calculated as a function of the dynamic temperatures of the power transformer, as expressed by (4).

$$LL = f_{PW}PW + f_{PE}PE + f_{S}P \tag{4}$$

The temperature of the winding has a direct impact on the load losses of the equipment due to the variation of the resistivity. To illustrate this phenomenon let us consider a 100 MVA transformer and apply (5), (6), and (7) at 75 °C. In this case, the Ohmic losses are 264.274 kW, the winding eddy losses are 33.630 kW and the stray losses are 39.206 kW. However, if the reference temperature changes to 45 °C, the Ohmic losses become 238.658 kW, the winding eddy losses become 30.370 kW and the stray losses become 43.414 kW. Thus, the load losses at 75 °C are 397.11 kW while the load losses at 45 °C are 372.442 kW or 7.8% lower, i.e. this shows the importance of loss correction for the ambient temperature change and the actual temperature of the loading cycle.

The fitted equation is defined according to the points obtained in the optimization process for resistivity winding losses (PW), where the coefficient of determination R^2 is determined as follows:

$$PW = 20.454 S_{input}^2 - 1682.2 S_{input} + 227954 \quad (5)$$

Based on the optimization points, Eq. (6) is fitted for the winding eddy losses parameters, in which R^2 is 0.9704. This coefficient represents the proportion or relationship between the dependent variable PW and the remaining parameters of the function (independent variables). In this case, R^2 indicates approximately 95.72% of the variability in the resistivity winding losses, 97.04% in the winding eddy losses, and 98.42% in the stray losses.

$$PE = 33454 \ln(S_{input}) - 120431 \quad (6)$$

Eq. (7) is obtained by fitting the function from the points defined by the optimization process for the stray losses parameters PS, with the coefficient R^2 equal to 0.9842.

$$PS = 1.1896 \cdot S_{input}^2 + 541.22 \cdot S_{input} - 3019.4 \quad (7)$$

2.1. Transformer efficiency

The transformer efficiency is expressed from the relationship between the output power S_{out} and the input power S_{in}:

$$\eta = 100 \frac{S_{out}}{S_{in}} \quad (8)$$

The transformer efficiency at any operating point (9), is calculated as a function of no-load losses at rated voltage and frequency P_0, short circuit losses at the rated current and reference temperature P_{SC}, load factor k and the rated apparent power of the transformer S_r.

$$\eta = 100\left(1 - \frac{k^2 P_{SC} + P_0}{S_r + P_0 + k^2 P_{SC}}\right) \quad (9)$$

The load losses are expressed by (10).

$$P_k = k^2 P_{SC} \quad (10)$$

The output power P_{out} is calculated by (11).

$$P_{out} = k S_{out} \cos\phi \quad (11)$$

where $\cos\phi$ is the load power factor. The maximum efficiency η_{max} is obtained when the no-load losses are equal to the load losses as shown in (12) and (13).

$$\eta_{max}(k_{opt}) \longrightarrow P_k = P_0 = k^2 P_{SC} \quad (12)$$

$$k_{opt} = \sqrt{\frac{P_0}{P_{SC}}} \quad (13)$$

Substituting the load index for optimal value in (9), it is possible to determine the PEI. Assuming the power factor as a per-unit value, a population of specific transformers might be compared. The maximum efficiency occurs when $P_k = P_0$. This way (9) can be restructured as (14).

$$PEI = \eta_{max} = 100\left(1 - \frac{2P_0}{k_{opt} S_r + 2P_0}\right) \quad (14)$$

PEI is a function of P_0, P_{SC}, S_r and the power factor of the load $\cos\phi$. This approach is useful for the comparison of the energy efficiency of large distribution transformers to different primary voltage, which is applied in energetic studies of installed transformers samples. This method focuses on the specific design concept of each transformer unit in terms of component losses.

2.2. Economic analysis

The losses used for capitalization evaluation should include the cooling losses, i.e. energy consumed by the cooling equipment during the operation. Such power consumption can appear when the transformer is operating with no-load losses or with both, with and without load losses. The Total Cost of Ownership TCO is calculated by (15), where terms IC is the initial cost of the power transformer and P_{Co} is the cooling power for no-load operation.

$$TCO = IC + A(P_0 + P_{Co}) + B(P_{SC} + P_{CS} - P_{Co}) \quad (15)$$

2.3. Temperature correction

The load factor is one of the critical indicators needed for transformer specification and can be defined using either the average load or the average overtime of the root mean square (RMS) value of the instantaneous load [32,33]. This work proposes a novel approach for the correction of the RMS load based on the transformer winding temperature, where the temperature correction factor is taken into account.

The mean winding temperature is usually specified as a temperature rise, but actual load losses are calculated at absolute temperature, therefore, the ambient temperature has a direct influence on the load losses. There are two standard values indicative of the "mean winding temperature": 55 °C temperature rise for non-thermally upgraded paper and 65 °C temperature rise for the thermally upgraded paper. According to [34], the ambient temperature is fixed at 20 °C, and in order to compare the load losses we need to choose a reference temperature. Typically, 75 °C or 85 °C are used as reference temperatures the load loss values are warranted at a reference load and temperature. This study uses load loss correction at the actual temperature instead of a reference temperature.

Fig. 2 shows a simulation with 85 °C as losses reference and the real temperature profile. It is observed that the losses are highly dependent on the temperature, the optimal transformer size can be determined by comparing these two results. The losses vary with the load profile during a determined time period, and the load factor L_f can now be represented as the average overtime of the root mean square RMS values of the instantaneous load considering instantaneous temperature correction.

The average loading is described as the annual load average and the load factor L_f is calculated by (16).

$$L_f = \frac{1}{h} \int_0^h f_{load}\, dt \quad (16)$$

where f_{load} is the time function represented in Fig. 2, in which the load loss factor is calculated from a definite integral throughout a year (total period), where h is the number of hours in one year.

Average RMS overtime represents a more suitable method for intermittent energy sources. The load loss factor L_f is given by (17).

$$L_f = \sqrt{\frac{1}{h} \int_0^h f_{load}(t)^2 dt} \quad (17)$$

Finally, the conventional expression of the loading function in (17) is reformulated taking into account the temperature correction f_{temp} as in (18).

$$L_f = \sqrt{\frac{1}{h} \int_0^h f_{temp}(t)^2 dt} \quad (18)$$

In sequence, Fig. 3 shows the flowchart of the proposed methodology. The proposed method calculates the maximum hotspot and top oil temperature considering the loading profile, as well as equivalent aging. The algorithm verifies if these three outputs exceed the limit imposed by the well-established international standards. If no constraints are found, a reduction of 1 MVA in the total size of the transformer is

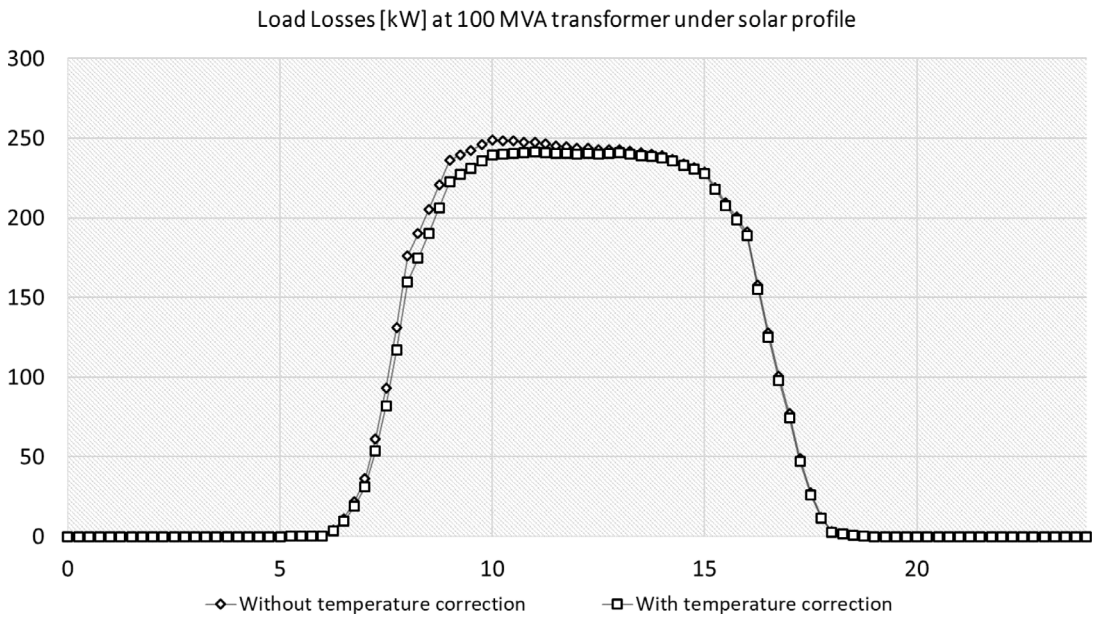

Fig. 2. Comparison of load losses with and without temperature correction.

performed and the iterative process continues. Otherwise, the algorithm stops and shows the latest calculation value of the power, following these three criteria. The ambient temperature T_{amb} is a time-dependent variable, which represents an array of values. The maximum step considered is one hour, i.e. temperature measurements are collected hourly and input into the optimization algorithm. The loading curve applied to the generator step-up (GSU) collector transformer throughout an entire year is also a time-dependent function, which represents one of the most important and sensitive input information in the proposed model. In addition, the maximum hotspot (HS) and the maximum top oil (TO) temperature limits are needed in the optimization algorithm. Both hotspot and top oil are considered long-time emergency loading instead of normal cycle, since the total time with solar radiation during a day is less than 24 hours, but more than a few minutes. Long-time emergency loading permits the hotspot and top oil temperature to exceed the normal cyclic temperatures and may be applied to transformers carrying non-continuous loads. In this research, the temperature limits established in the IEEE guide are considered, i.e. 140 °C for the hotspot and 110 °C for the top oil temperature. These temperature values are defined by the thermal limits of the mineral oil and thermally upgraded insulation paper [34]. In the case of high-temperature class materials, such as aramid paper and/or ester fluid, these values can be increased and therefore the transformer size can be reduced. The loss of insulation life must also be quantified as less than 1.0 p.u. equivalent aging EQ_{aging}. As long as none of HS_{output}, TO_{output} or EQ_{aging} exceed the maximum value allowed, the proposed optimization technique reduces the total size by 1 MVA until it converges to the optimum transformer size, which fulfills all restrictions and prior established constants.

3. Case study

Initially, a general overview of the PV farm and electric power grid is shown in Fig. 4, where a GSU transformer is connected between both systems. The common technical characteristics of the power transformer are described in the Table 1.

Fig. 5 represents the per unit load of a solar profile. The data in Fig. 5 is collected during one year considering the solar radiation of the 8760 hours with one-minute time-step and 525600 total number of points.

Fig. 6 shows the load factor calculated by using the three different methods. For a 100-MVA generator step-up (GSU) transformer, the

Table 1
Transformer parameters.

Rated power, [MVA]	55–100
High voltage, [kV]	230 ± 10% with tap changer
Low voltage, [kV]	34.5
Cooling impedance, [%]	12
Max. total losses (ONAF), [%]	0.4
Connection	Ynd1
No-load losses capitalization, [USD/kW]	2500
Load losses capitalization, [USD/kW]	2500
Loading profile	1.0 p.u. (flat curve)
Ambient temperature, [°C]	30 (continuous)
Max. hotspot rises, [°C]	80
Max. top oil rises, [°C]	65
Max. mean winding rises, [°C]	65
Type of oil	Mineral
Solid insulation material	Thermo-established paper
Winding conductor material	Copper
Total lifetime considered, [h]	150000 [34]

average loading based on the solar energy profile in Fig. 5 is around 58.9%, in which the conventional RMS overtime is 50.4% and 51.2% for RMS with temperature corrections. Smaller power transformers, such as 55 MVA, have an average load factor smaller than 80%, while for RMS load factor without temperature correction, this value is 98%, and for RMS load factor with temperature correction 93.1%. When connected to solar power production, this power transformer rarely reaches the rated loading factor and the hotspot of 85 °C, due to the large load variation. Therefore, when temperature correction is applied a bigger gap appears for smaller equipment due to higher temperature of operation.

Loading profile and ambient temperature are key real-time parameters for establishing dynamic transformer rating. The average ambient temperature mapping and average load represent typical yearly behavior of a largely urban and industrial area in South America. Please note that the summer season is from December to March in the Southern Hemisphere. Therefore, more power demand is required for residential and commercial air-conditioning as well as many other cooling applications. An annual distribution of daily average temperature is presented in Fig. 7. Higher temperatures are observed around 13 up to 15 hours and the highest ambient temperatures throughout the year occur in January/February and November/December. At the same time, during

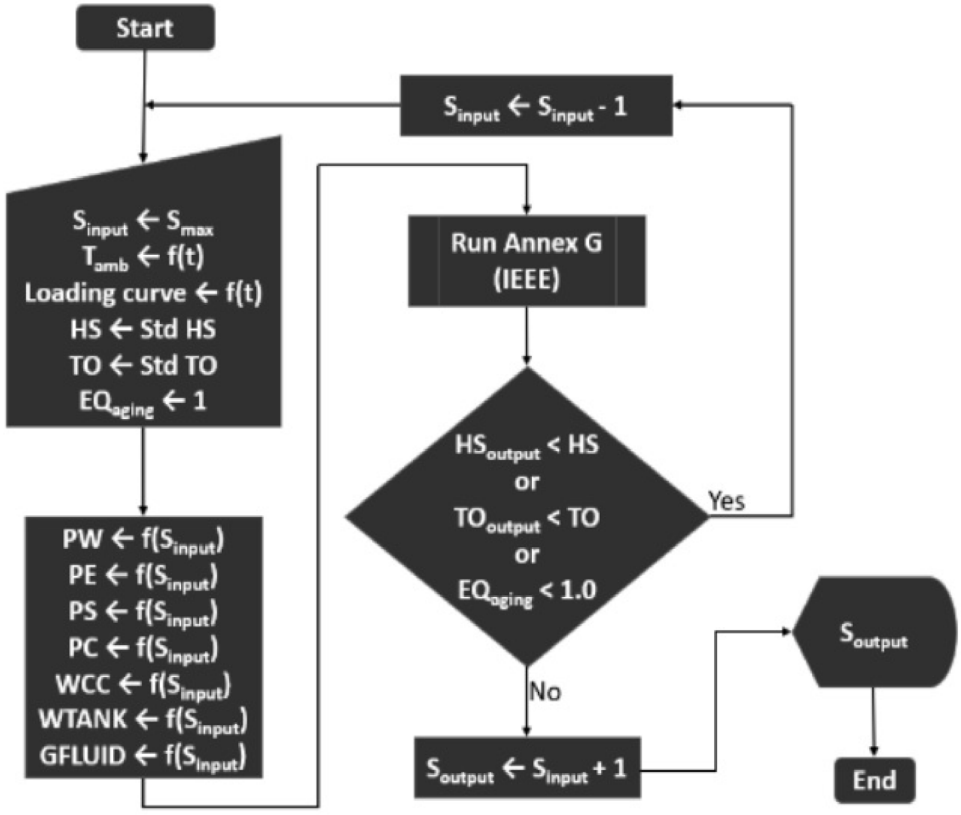

Fig. 3. Proposed optimization methodology.

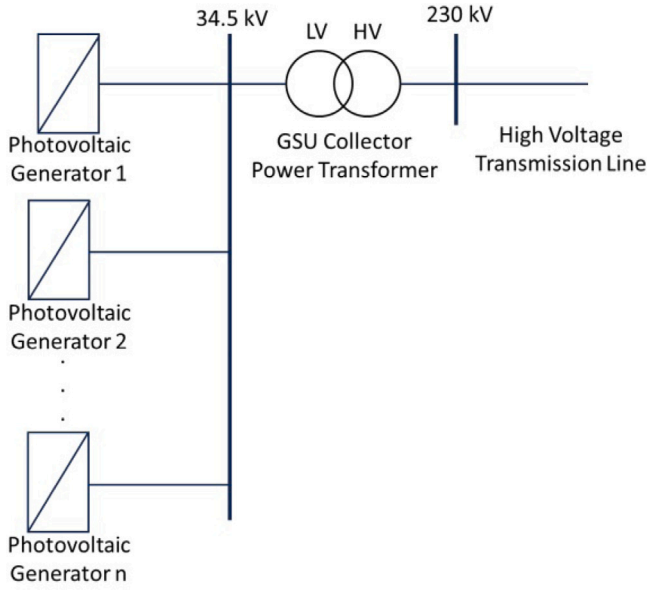

Fig. 4. PV farm connected to the electric power grid.

these months transformer experiences the highest level of loading as shown in Fig. 8.

According to Fig. 8, the absolute maximum generation of the solar power plant is equal to 1.0 p.u. and the maximum average of 0.98 p.u. occurs at 10:00 A.M. in December, i.e. the intermittent behavior of photovoltaic power generation demands the transformer to operate at rated load only a few hours per year.

Annual load distribution for 100 MVA transformer as shown in Fig. 9 is obtained by using data from Figs. 7 and 8 as inputs to the loading curve calculations according to the IEEE bottom-oil model [34]. The blue curve in Fig. 9 represents the average loading profile where the maximum load does not exceed 0.9 p.u.; the grey curve is the dynamic profile of the hotspot temperature of the transformer, with a maximum value of ≈ 80 °C. Top oil and bottom oil temperatures are represented by yellow and green colors respectively and the orange bars show the corresponding ambient temperatures.

The following operation parameters are identified using Fig. 9:

- Maximum hotspot temperature is equal to 79.84 °C at 15 h and 00 min;
- Maximum top fluid temperature is equal to 64.35 °C at 15 h and 21 min;
- Equivalent aging rate is 0.178805 p.u. for 10 min and 44 s a day.

A transformer with thermally upgraded paper is designed to withstand hotspot temperature of 110 °C for the entire duration of its lifetime [34, 35], which means that at 110 °C, the equivalent aging factor for transformer insulation is a unitary value, i.e., after 150,000 h the DP of the paper will reach the end-of-life criteria.

Fig. 10 shows the calculated values of the hotspot absolute temperature, top oil absolute temperature, and equivalent aging in hours.

Thereafter, determining the minimum and technically viable size of the power transformer, the formulation of the loss's capitalization is applied to determine the minimum TOC.

Firstly, technical analysis is carried out and the minimum rated power possible is found which meets all technical specifications. After the technical optimization, a financial comparison is started to calculate the TOC, i.e., the optimum transformer size from the technical point of view can be or not be the optimum point from the technical plus financial itself.

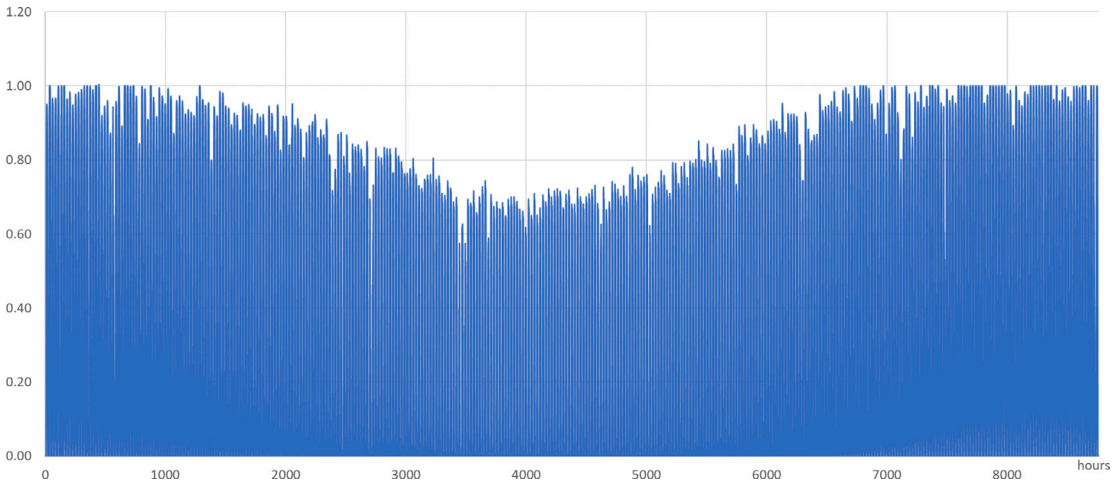

Fig. 5. Per unit solar radiation along the year.

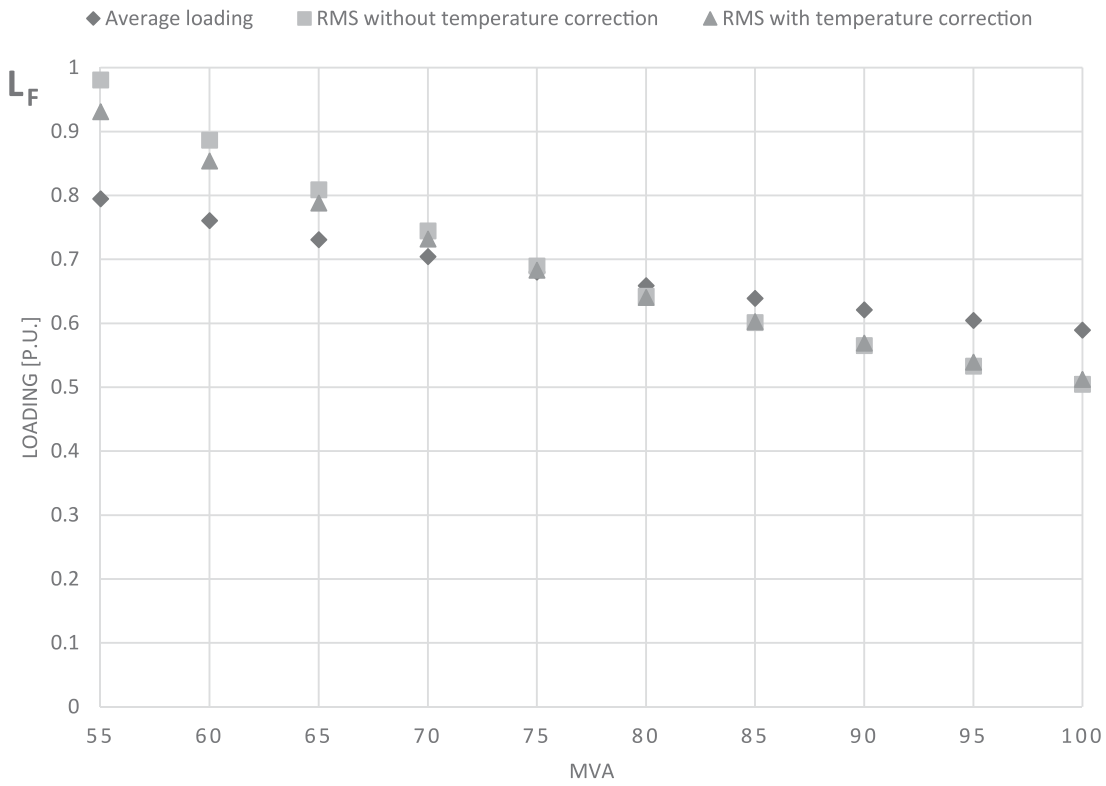

Fig. 6. Load loss factor versus transformer size.

Fig. 11 shows the transformer temperatures, and the ambient temperature, and the dotted curve represents the average winding temperature. From Fig. 11, it is possible to observe that winding thermal inertia is higher than the thermal inertia of the transformer as a whole. The thermal stability for this transformer cannot be achieved with the loading profile of a solar plant.

3.1. Investment parameters

To simulate the real case and calculate the TOC to compare RMS load approaches with and without temperature correction the sensitivity analysis is performed. The average energy price of the first year of operation of a solar plant is 0.02033 USD/kWh according to Fig. 12. The average annual increase in energy cost is 1.52% per year according to a weighted index of the energy price shown in Fig. 13 [36]. From 2020 to 2030, the average increment is from 72.0 to 87.2 USD, therefore, the annual average increase in estimated price is 1.52% per year for the next 10 years. Another important factor is the weighted average cost of capital (WACC), which is 6.6% per year for power utilities [37].

The total cost of transformer installation and commissioning is highly correlated with the prices of materials used in the manufacturing process. Therefore, a good estimate of the initial investment price (IP) is the costs of the most used materials in transformer manufacturing as given by (19).

$$IP = f_{price}(m_{copper}w_{copper} + m_{iron}w_{iron} + m_{oil}w_{oil}) \tag{19}$$

where, f_{price} is the price factor, which is used for considering all other potential elements, a chosen price factor is 2.8 [USD/kg]; m_{copper} is the total mass of the copper, [kg]; w_{copper} is the price of the copper,

	Average - Temperature [°C]												
h	Jan	Feb	Mar	Apr	May	Jun	Jul	Aug	Sep	Oct	Nov	Dec	Annual
0	13.39	13.85	13.52	12.00	10.06	8.88	7.66	8.82	9.01	9.95	10.85	12.07	10.82
1	12.71	13.16	12.94	11.32	9.30	7.96	6.67	7.71	8.02	8.96	10.04	11.32	9.99
2	12.03	12.48	12.37	10.64	8.54	7.06	5.69	6.63	7.08	7.97	9.23	10.58	9.17
3	11.35	11.80	11.80	9.96	7.79	6.18	4.70	5.57	6.16	6.98	8.42	9.83	8.36
4	10.66	11.12	11.23	9.28	7.02	5.33	3.76	4.57	5.27	6.04	7.61	9.15	7.57
5	10.10	10.43	10.66	8.60	6.26	4.53	2.83	3.69	4.44	5.22	6.80	8.51	6.82
6	10.75	10.14	10.08	7.92	5.52	3.76	2.18	2.97	3.86	6.29	8.80	10.07	6.84
7	12.30	12.17	11.89	9.45	6.48	3.81	2.14	3.98	6.89	8.75	10.96	11.89	8.37
8	14.07	13.93	13.61	11.59	8.97	6.75	5.66	6.96	9.85	11.43	13.15	13.76	10.79
9	15.78	15.66	15.30	13.68	11.55	9.89	9.15	10.32	12.71	13.97	15.17	15.57	13.21
10	17.34	17.23	16.81	15.59	13.89	12.84	12.36	13.41	15.32	16.22	16.94	17.17	15.41
11	18.65	18.57	18.07	17.17	15.89	15.32	15.10	16.00	17.46	18.08	18.36	18.47	17.25
12	19.71	19.63	19.05	18.38	17.42	17.21	17.22	17.99	19.08	19.50	19.42	19.48	18.67
13	20.46	20.39	19.72	19.15	18.39	18.40	18.62	19.28	20.13	20.43	20.12	20.16	19.60
14	20.86	20.81	20.06	19.49	18.81	18.91	19.26	19.90	20.59	20.87	20.43	20.49	20.03
15	20.97	20.91	20.07	19.37	18.59	18.66	19.05	19.83	20.41	20.80	20.36	20.49	19.95
16	20.66	20.57	19.58	18.62	17.54	17.42	17.71	18.71	19.33	19.96	19.70	20.02	19.15
17	19.90	19.76	18.64	17.31	15.86	15.34	15.46	16.71	17.47	18.47	18.50	19.07	17.70
18	18.76	18.56	17.39	16.35	15.01	14.39	14.39	15.50	15.59	16.57	16.92	17.77	16.42
19	17.52	17.74	16.72	15.57	14.16	13.44	13.31	14.29	14.45	15.41	15.88	16.79	15.43
20	16.63	16.91	16.04	14.80	13.31	12.49	12.24	13.08	13.30	14.26	14.85	15.81	14.46
21	15.74	16.09	15.37	14.03	12.46	11.54	11.17	11.86	12.19	13.10	13.81	14.83	13.50
22	14.88	15.26	14.69	13.25	11.61	10.59	10.10	10.65	11.07	11.95	12.77	13.85	12.54
23	14.01	14.44	14.01	12.48	10.76	9.64	9.03	9.44	9.96	10.79	11.73	12.87	11.58

Fig. 7. Annual average temperature.

	Average - Load												
h	Jan	Feb	Mar	Apr	May	Jun	Jul	Aug	Sep	Oct	Nov	Dec	Annual
0	0.00000	0.00000	0.00000	0.00000	0.00000	0.00000	0.00000	0.00000	0.00000	0.00000	0.00000	0.00000	0.00000
1	0.00000	0.00000	0.00000	0.00000	0.00000	0.00000	0.00000	0.00000	0.00000	0.00000	0.00000	0.00000	0.00000
2	0.00000	0.00000	0.00000	0.00000	0.00000	0.00000	0.00000	0.00000	0.00000	0.00000	0.00000	0.00000	0.00000
3	0.00000	0.00000	0.00000	0.00000	0.00000	0.00000	0.00000	0.00000	0.00000	0.00000	0.00000	0.00000	0.00000
4	0.00000	0.00000	0.00000	0.00000	0.00000	0.00000	0.00000	0.00000	0.00000	0.00000	0.00000	0.00000	0.00000
5	0.00000	0.00000	0.00000	0.00000	0.00000	0.00000	0.00000	0.00000	0.00000	0.00000	0.00000	0.00000	0.00000
6	0.04320	0.00128	0.00000	0.00000	0.00000	0.00000	0.00000	0.00000	0.00011	0.06357	0.17788	0.14437	0.03606
7	0.56622	0.38394	0.25553	0.13740	0.03921	0.00074	0.00079	0.06273	0.33777	0.66302	0.77259	0.72366	0.32836
8	0.85470	0.80368	0.75843	0.67256	0.57210	0.43960	0.45061	0.62905	0.78625	0.89257	0.92994	0.89028	0.72283
9	0.93673	0.90655	0.87848	0.78989	0.69243	0.64748	0.66558	0.77556	0.87863	0.94621	0.97252	0.96354	0.83741
10	0.96434	0.93647	0.90481	0.81875	0.70951	0.68348	0.69645	0.79714	0.89035	0.95442	0.97861	0.98066	0.85913
11	0.95732	0.94619	0.90864	0.81845	0.71672	0.67459	0.69485	0.78907	0.88512	0.95248	0.96806	0.97365	0.85659
12	0.96022	0.94383	0.90553	0.81061	0.70947	0.66205	0.68671	0.77545	0.87561	0.94644	0.96000	0.97284	0.85022
13	0.95948	0.94246	0.90657	0.80350	0.70598	0.66427	0.68643	0.77404	0.87352	0.94324	0.96285	0.96677	0.84858
14	0.93665	0.93698	0.90026	0.79650	0.70577	0.66826	0.68971	0.77401	0.86920	0.93175	0.95171	0.95313	0.84229
15	0.92526	0.91725	0.88529	0.77295	0.67949	0.65578	0.67323	0.76337	0.85362	0.90516	0.93793	0.92506	0.82398
16	0.86955	0.87086	0.83096	0.70348	0.58211	0.54831	0.59720	0.68809	0.78220	0.82933	0.87132	0.86727	0.75272
17	0.74038	0.74810	0.64593	0.37144	0.16359	0.11383	0.20198	0.33402	0.45888	0.56118	0.69375	0.72394	0.47832
18	0.33407	0.27612	0.09201	0.00033	0.00000	0.00000	0.00000	0.00000	0.00091	0.03193	0.12843	0.25443	0.09235
19	0.00000	0.00000	0.00000	0.00000	0.00000	0.00000	0.00000	0.00000	0.00000	0.00000	0.00000	0.00000	0.00000
20	0.00000	0.00000	0.00000	0.00000	0.00000	0.00000	0.00000	0.00000	0.00000	0.00000	0.00000	0.00000	0.00000
21	0.00000	0.00000	0.00000	0.00000	0.00000	0.00000	0.00000	0.00000	0.00000	0.00000	0.00000	0.00000	0.00000
22	0.00000	0.00000	0.00000	0.00000	0.00000	0.00000	0.00000	0.00000	0.00000	0.00000	0.00000	0.00000	0.00000
23	0.00000	0.00000	0.00000	0.00000	0.00000	0.00000	0.00000	0.00000	0.00000	0.00000	0.00000	0.00000	0.00000

Fig. 8. Annual average load.

[USD/kg]; m_{iron} is the total mass of iron, [kg]; w_{iron} is the price of iron, [USD/kg]; m_{oil} is the total mass of oil, [kg] and w_{oil} is the price of cooper, [USD/kg].

The materials have variable prices, therefore, the chosen prices are approximated from the current market value. The input data used in this study is summarized below:

- Average energy price of the first year in operation 0.02033 USD/kWh;
- Average annual increase in energy cost rated of 1.52%;
- Number of years before the invested amount shall be paid back: 17.12 years which is equivalent to 150.000 hours;
- Weight average cost of capital of 6.6%;
- Copper cost: 8.0 USD/kg;
- Iron cost: 2.0 USD/kg (electrical steel core material);
- Oil cost, : 1.0 USD/kg;
- Factor price, $f_{price} = 2.8$.

4. Results

The total cost of ownership is calculated according to (15). Table 2 shows the TOC calculated, in kUSD, by using the three methods introduced previously in this section. Table 2 shows that there is a different optimum point when temperature correction is considered. The first row shows the initial cost calculated using (19) and the smaller the transformer is, the lower the initial prices. When TOC is calculated is it possible to observe that, there is a minimum optimum transformer size. The green color means the lower TOC prices and the red color shows the higher TOC. For the RMS approach without temperature correction, the optimum point is a transformer with 80 MVA rated power and TOC equal to 733 kUSD, and when the temperature correction is considered a 75 MVA transformer is encountered with 731 kUSD. The minimum allowable transformer size is 68 MVA due to the technical limitations of aging, top oil, and hotspot temperature. If only technical limitations are taken into account, the 68 MVA transformer should be chosen. If

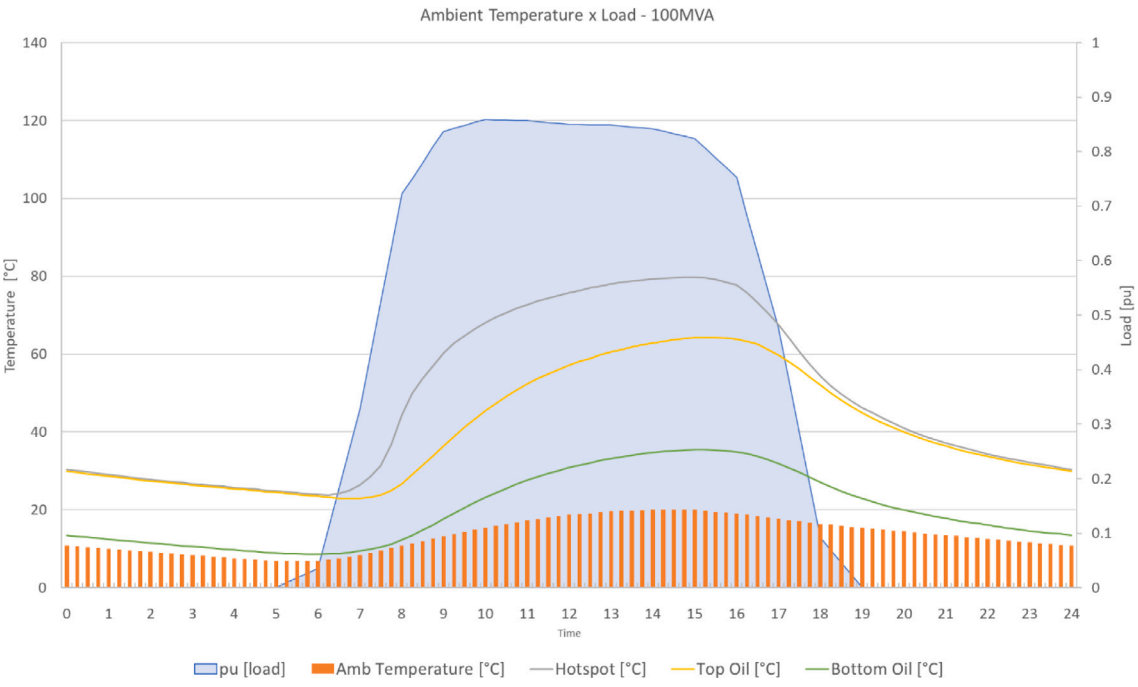

Fig. 9. Annual average loading and temperatures for a 100 MVA transformer.

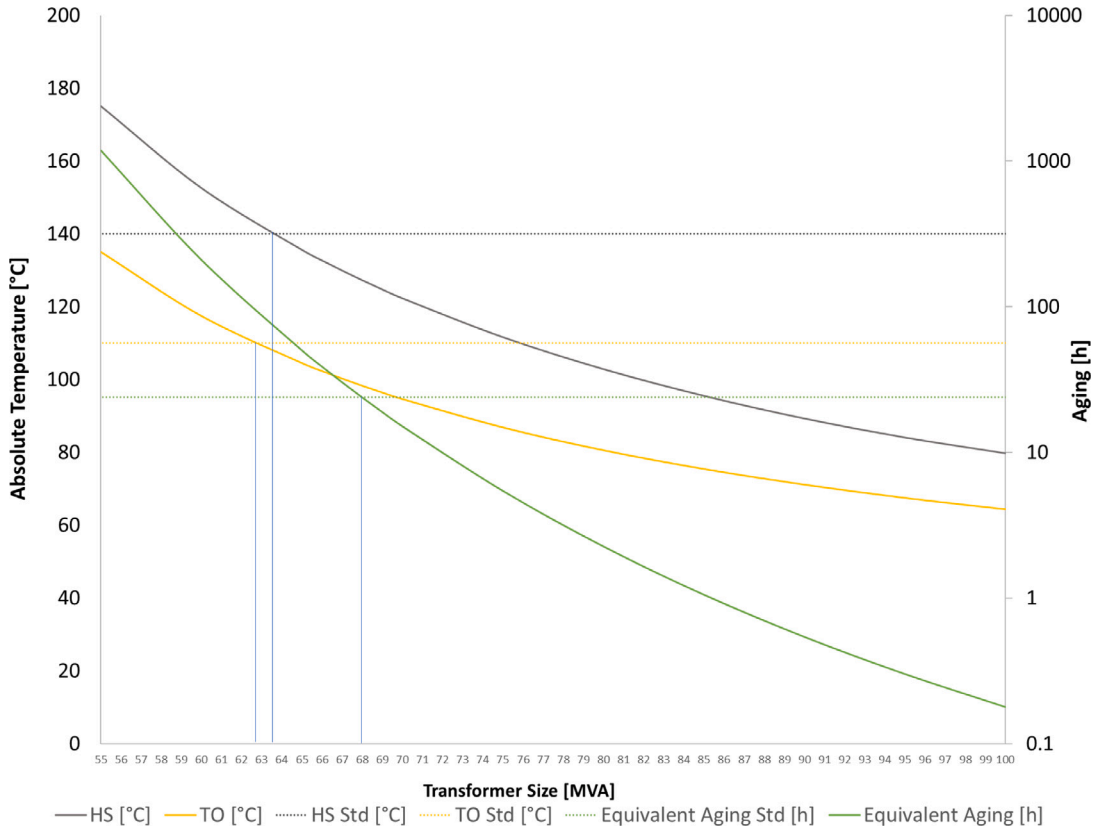

Fig. 10. Absolute temperature of hotspot and top oil, and equivalent aging limits.

all the criteria are taken into account the 75 MVA transformer is the optimal choice.

Fig. 14 shows the efficiency index comparing two different approaches with and without temperature correction and the peak efficiency index, PEI, which is obtained when the no-load losses are equal to the load losses calculated using (14).

A more realistic data of the efficiency index is presented in Fig. 14 when the calculation considered a specific loading of the transformer, in this case, it is the real load loss factor calculated for each approach, i.e., for 75 MVA transformer the RMS without temperature correction is 68.96% and with temperature correction is 68.30%.

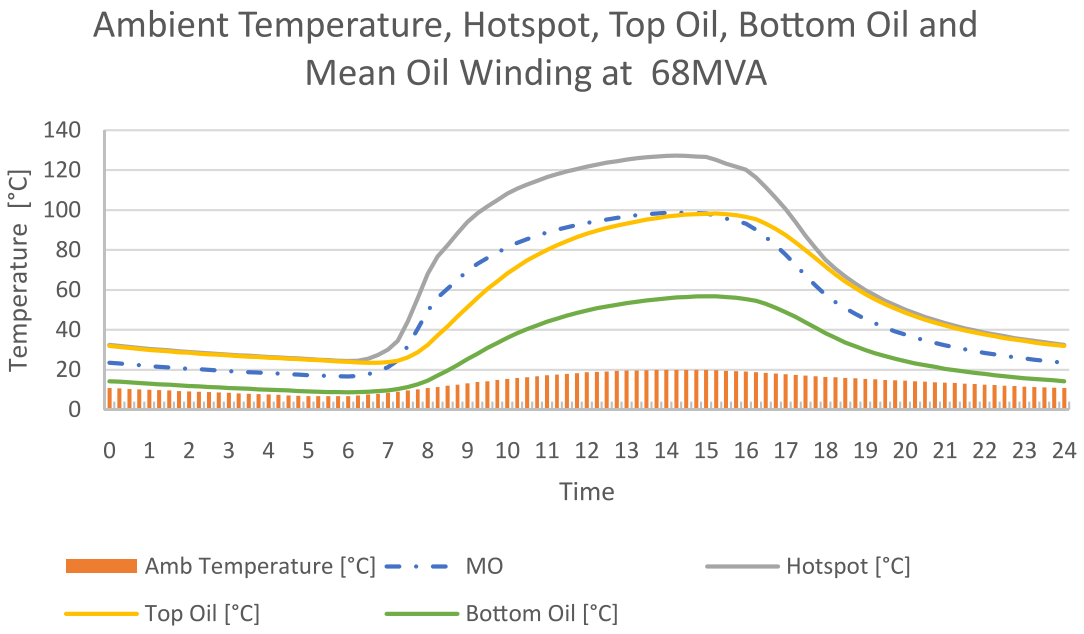

Fig. 11. Ambient temperature and temperatures inside the 68 MVA transformer.

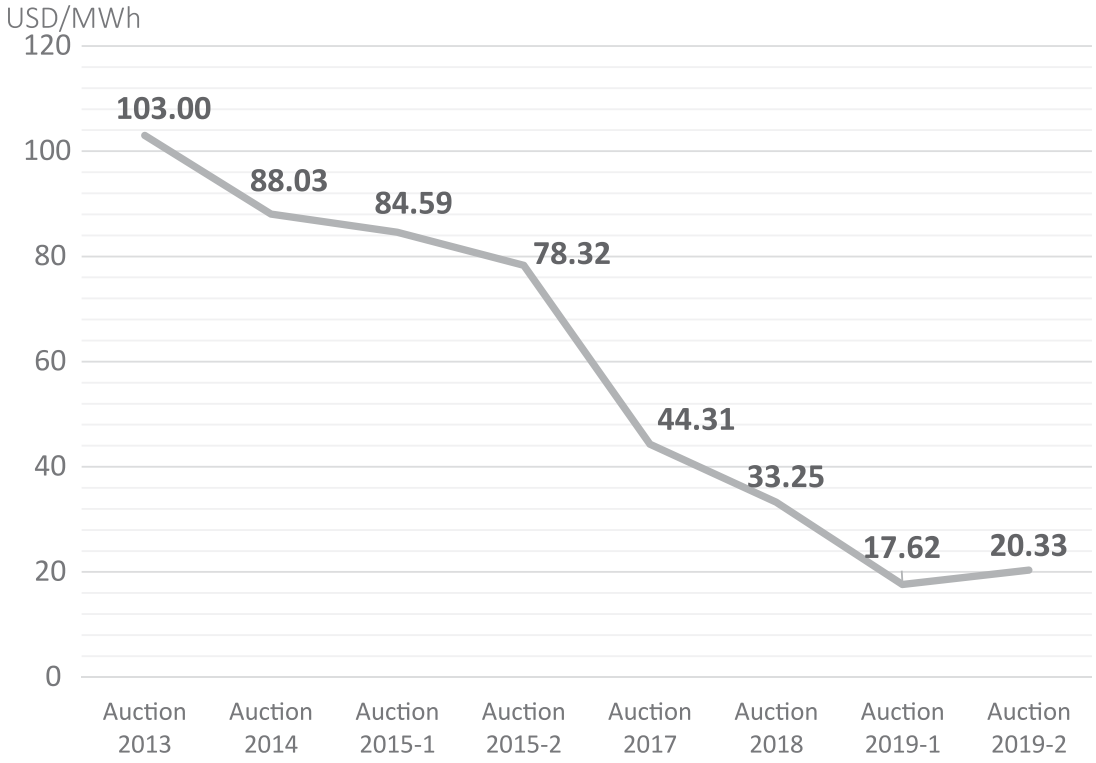

Fig. 12. Prices evolution during auction in Brazilian regulated market [38].

Table 2
Initial Cost and TOC versus transformer size using RMS approaches with and without temperature correction.

Power, [MVA]	100	95	90	85	80	75	70	65	60	55
Initial Cost [kUSD]	444	429	413	396	379	361	343	324	304	284
TOC [kUSD] - RMS	751	744	738	734	733	737	745	762	791	837
TOC [kUSD] - RMS with temperature correction	757	748	741	735	732	731	735	745	763	792

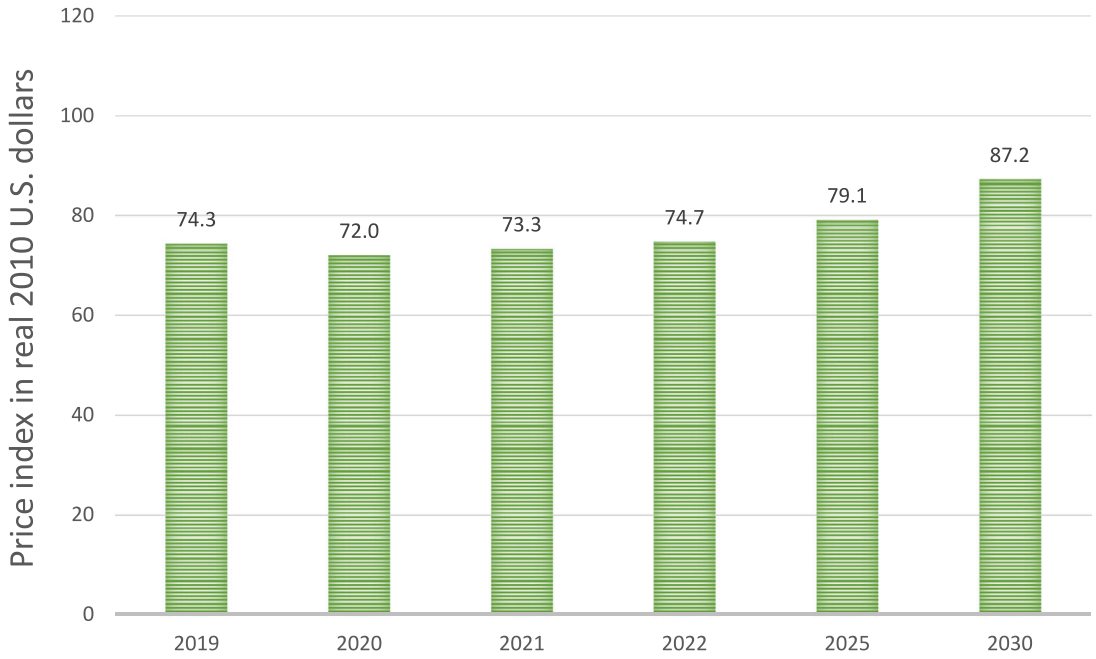

Fig. 13. Price index of energy worldwide from 2019 to 2030 in U.S. dollars, price index in 2010 [36].

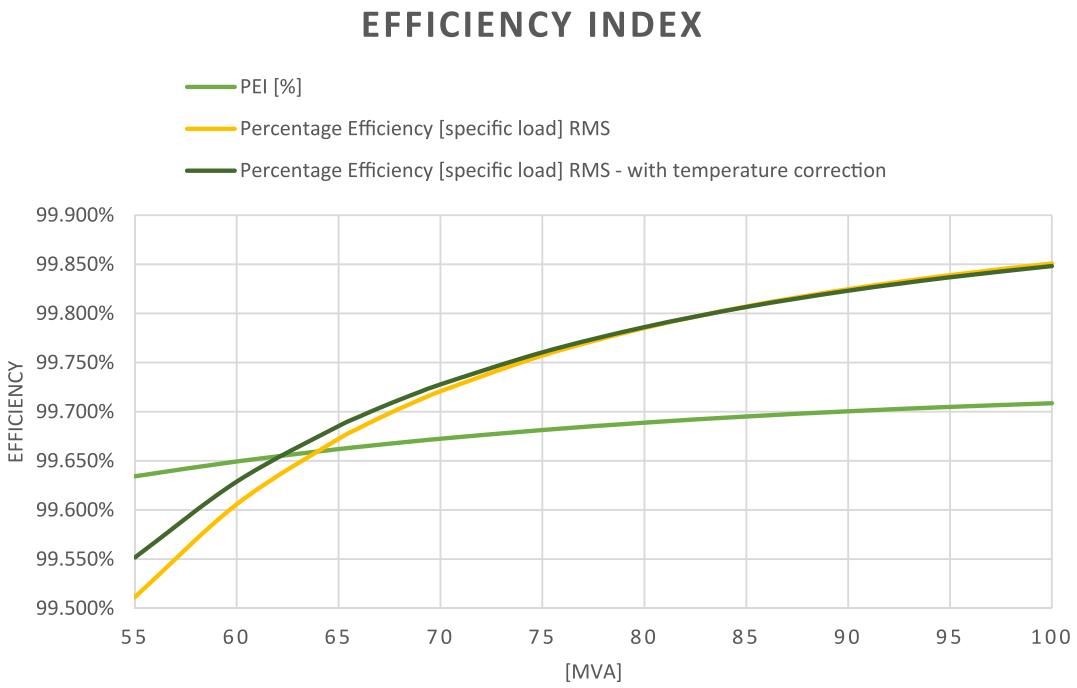

Fig. 14. Efficiency index of specific load and PEI.

In this example, for RMS with temperature correction higher index compared with PEI is seen when the chosen transformer is bigger than 63 MVA. The PEI has a lower index because this index is calculated when the no-load losses are equal to the load losses per definition, i.e., in power transformer units it usually occurs at low load which makes this transformer with high efficiency at low loads. The proposed method also increases the transformer efficiency at the specific load which this equipment will operate along the entire year, becoming more compact and efficient.

It is possible to reduce the total rated power by 25%, from 100 MVA to 75 MVA when the new approach is applied. The no-load losses are reduced from 63.3 kW to 52.9 kW as presented in Table 3. The load losses are higher in this case, because the quantity of cooper material is approximately 19% lower, but the 75 MVA transformer operates below 20% at overload conditions. Comparing the no-load loss, from 100 MVA to 75 MVA the no-load losses came from 63.3 kW to 52.9 kW, a reduction of 19.6% of losses for the total transformer lifetime.

4.1. Real loading curve with reactive dispatch - example

The approach considering reactive power dispatch is presented further. The quantity of the reactive power dispatch is shown in Fig. 15,

Table 3
Mass and losses comparison.

Power [MVA]	Core [kg]	No-load losses [kW]	Cooper [kg]	Load losses at 100 MVA [kW]
65	75%	48.3	72%	595.0
70	78%	50.6	76%	533.0
75	82%	52.9	81%	483.1
80	82%	55.0	85%	442.4
85	90%	57.2	89%	408.8
90	93%	59.3	93%	380.7
95	97%	61.3	97%	357.1
100	100%	63.3	100%	337.1

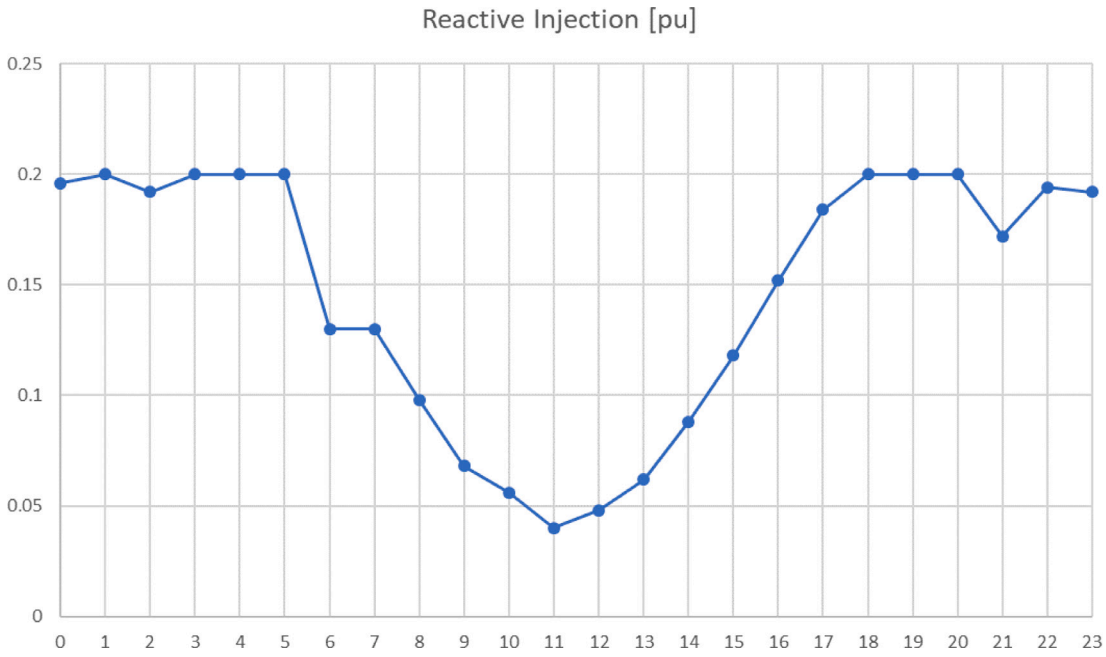

Fig. 15. Example of a reactive injection on the grid in a solar power plant.

Table 4
Initial Cost and TOC versus transformer size using RMS approaches with and without temperature correction adding the reactive dispatch.

Power, [MVA]	100	95	90	85	80	75	70	65	60	55
Initial Cost [kUSD]	444	429	413	396	379	361	343	324	304	284
TOC [kUSD] - RMS	812	809	808	810	817	830	851	883	933	1008
TOC [kUSD] - RMS with temperature correction	817	812	809	808	811	818	831	851	883	930

which shows that approximately all reactive power is dispatched during night-time and early morning [39]. Considering the dispatch of reactive power in a photovoltaic power plant it is observed that there is an increase in the load of the transformer that will operate in the substation. Fig. 16 shows the average load curve of the loading of the transformer.

The TOC for this scenario is presented in Table 4.

In the case of the same equipment for the reactive injection, it is necessary to acquire equipment with at least 85 MVA of power to ensure that all the criteria are satisfied. Such analysis is of paramount importance for the purchaser of the equipment, since if the equipment is dimensioned or does not consider the use of reactive power, the useful life of the equipment can be reduced considerably.

5. Conclusion

The increasing integration of intermittent power sources in the grid has required more sophisticated techniques during the project and manufacturing of power equipment in financial and technical terms. This paper has addressed yet unresolved issues on how to optimize transformer size for new solar power plants as a function of the expected power generation curve and environment temperature. Such power transformers will operate throughout their Life cycle while fulfilling all economic criteria, ultimately achieving the most cost-effective transformer solution. After an in-depth review of the technical literature, only a few researches were found on the proposed subject. However, such research does not take into account the temperature

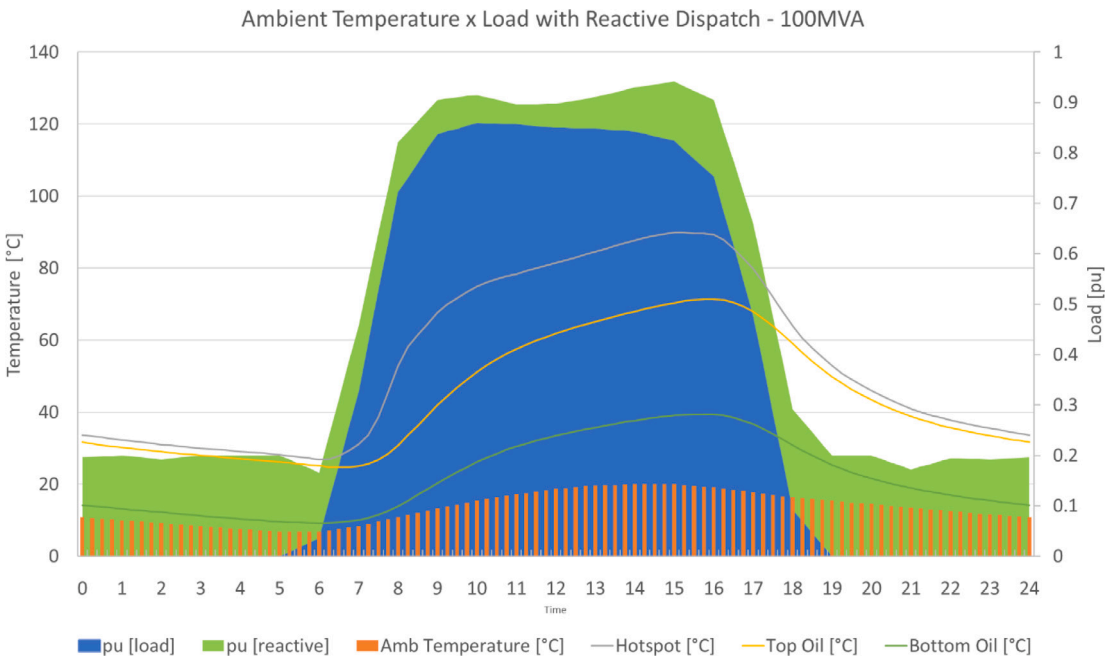

Fig. 16. Annual average loading and temperatures for a 100-MVA transformer and the average reactive power dispatch.

correction inside the winding, and neither does a joint relationship on the total ownership cost of the power transformer. In this sense, the proposed method showed to be efficient, because it can determine the most suitable equipment based on financial and technical information, such as the price of energy, WACC of the investor, transformer life expectancy, and others. The results and analyses showed the great potential to determine the project of the optimized transformer based on several variables and indexes, such as load factor, losses, solar radiation, transformer size, annual average ambient temperature and load varying, hotspots, and various pricing indexes. Such a method correlates all these features, which have not been previously found in the technical literature, and therefore represents an original contribution to assist the design of power transformers for systems with intermittent generation and loading. The results and conclusions provided in this research are relevant because manufacturers have reduced attention to loss capitalization, only focusing on the initial price of the transformer, or not distinguishing the difference between the capitalization of no-load losses and the capitalization of load losses. To avoid a reduction in the revenue of electricity production, a deep analysis in this context was carried out, which has demonstrated the importance of taking into account the loading profile and the huge difference between capitalization of no-load and load losses.

CRediT authorship contribution statement

Wílerson Venceslau Calil: Methodology, Formal analysis, Investigation, Visualization, Writing – original draft. **Kateryna Morozovska:** Writing – original draft, Writing – review & editing, Visualization. **Tor Laneryd:** Methodology, Validation, Resources, Writing. **Eduardo Coelho Marques da Costa:** Conceptualization, Methodology, Validation, Resources, Writing – revision, Supervision, Project administration. **Maurício Barbosa de Camargo Salles:** Conceptualization, Methodology, Validation, Resources, Writing – original draft.

Declaration of competing interest

The authors declare that they have no known competing financial interests or personal relationships that could have appeared to influence the work reported in this paper.

Data availability

The authors do not have permission to share data.

Acknowledgments

The authors would like to thank CAPES - Coordination for the Improvement of Higher Education Personnel and CNPq - Brazilian National Council for Scientific and Technological Development (Grant 25/2022).

The authors would like to thank Vinnova Program for Advanced and Innovative Digitalisation (Ref. Num. 2023-00241) and Vinnova Program for Circular and Biobased Economy (Ref. Num. 2021-03748) for partially sponsoring this work.

References

[1] B.D. Lahoti, D.E. Flowers, Evaluation of transformer loading above nameplate rating, IEEE Trans. Power Appar. Syst. PAS-100 (4) (1981) 1989–1998, http://dx.doi.org/10.1109/TPAS.1981.316554.

[2] M.F. Lachman, P.J. Griffin, W. Walter, A. Wilson, Real-time dynamic loading and thermal diagnostic of power transformers, IEEE Trans. Power Deliv. 18 (1) (2003) 142–148, http://dx.doi.org/10.1109/TPWRD.2002.803724.

[3] T. Zarei, K. Morozovska, T. Laneryd, P. Hilber, M. Wihlén, O. Hansson, Reliability considerations and economic benefits of dynamic transformer rating for wind energy integration, Int. J. Electr. Power Energy Syst. 106 (2019) 598–606, http://dx.doi.org/10.1016/j.ijepes.2018.09.038, URL http://www.sciencedirect.com/science/article/pii/S0142061517333033.

[4] P. Pacheco, M. Cuesto, M. Burgos, Sizing step-up transformers for solar generation based on load profiles predictability, in: 2019 6th International Advanced Research Workshop on Transformers, ARWtr, 2019, pp. 37–41, http://dx.doi.org/10.23919/ARWtr.2019.8930196.

[5] I.S. Benko, D.E. Cooper, D.O. Craghead, P.Q. Nelson, Loading of substation electrical equipment with emphasis on thermal capability part II-application, IEEE Trans. Power Appar. Syst. PAS-98 (4) (1979) 1403–1419, http://dx.doi.org/10.1109/TPAS.1979.319343.

[6] A.V. Turnell, A. Linnet, N. Tamadon, K. Morozovska, P. Hilber, T. Laneryd, M. Wihlen, E. Ab, Risk and economic analysis of utilizing dynamic thermal rated transformer for wind farm connection, in: 2018 IEEE International Conference on Probabilistic Methods Applied to Power Systems, PMAPS, 2018, pp. 1–6, http://dx.doi.org/10.1109/PMAPS.2018.8440479.

[7] I. Daminov, A. Prokhorov, R. Caire, M.C. Alvarez-Herault, Assessment of dynamic transformer rating, considering current and temperature limitations, Int. J. Electr. Power Energy Syst. 129 (3) (2021) 106886, http://dx.doi.org/10.1016/j.ijepes.2021.106886.

[8] G. Swift, T.S. Molinski, W. Lehn, A fundamental approach to transformer thermal modeling. I. Theory and equivalent circuit, IEEE Trans. Power Deliv. 16 (2) (2001) 171–175.
[9] D. Susa, M. Lehtonen, H. Nordman, Dynamic thermal modelling of power transformers, IEEE Trans. Power Deliv. 20 (1) (2005) 197–204.
[10] D. Susa, M. Lehtonen, Dynamic thermal modeling of power transformers: Further development-part I, IEEE Trans. Power Deliv. 21 (4) (2006) 1961–1970.
[11] D.A. Douglass, A.A. Edris, Real-time monitoring and dynamic thermal rating of power transmission circuits, IEEE Trans. Power Deliv. 11 (3) (1996) 1407–1418, http://dx.doi.org/10.1109/61.517499.
[12] L. Chittock, J. Yang, D. Strickland, C. Harrap, J. Mourik, Distribution network transformer thermal modelling parameter determination for dynamic rating applications, in: 8th IET International Conference on Power Electronics, Machines and Drives, PEMD 2016, 2016, pp. 1–6, http://dx.doi.org/10.1049/cp.2016.0296.
[13] J. Yang, D. Strickland, Thermal modelling for dynamic transformer rating in low carbon distribution network operation, in: 7th IET International Conference on Power Electronics, Machines and Drives, PEMD 2014, 2014, pp. 1–6, http://dx.doi.org/10.1049/cp.2014.0330.
[14] M. Akhlaghi, Z. Moravej, A. Bagheri, Flexible and sustainable scheduling of electric power grids: A dynamic line and transformer rating based approach under uncertainty condition, Sustain. Energy Grids Netw. 36 (2023) 101150, http://dx.doi.org/10.1016/j.segan.2023.101150, URL https://www.sciencedirect.com/science/article/pii/S2352467723001583.
[15] R. Karlsson, Power System Performance When Implementing Dynamic Rating on a Wind Farm Connected Transformer (Master's thesis), KTH, Electromagnetic Engineering, 2017, p. 59.
[16] K. Morozovska, R. Karlsson, P. Hilber, Dynamic rating of the wind farm transformer from the power system's perspective, in: 2021 IEEE Madrid PowerTech, 2021, pp. 1–6, http://dx.doi.org/10.1109/PowerTech46648.2021.9494902.
[17] J. Yang, L. Chittock, D. Strickland, C. Harrap, Predicting practical benefits of dynamic asset ratings of 33 kv distribution transformers, in: IET International Conference on Resilience of Transmission and Distribution Networks, RTDN 2015, 2015, pp. 1–6, http://dx.doi.org/10.1049/cp.2015.0898.
[18] T.S. Jalal, N. Rashid, B. van Vliet, Implementation of dynamic transformer rating in a distribution network, in: 2012 IEEE International Conference on Power System Technology, POWERCON, 2012, pp. 1–5, http://dx.doi.org/10.1109/PowerCon.2012.6401328.
[19] T.S. Jalal, Case study: Implementation of dynamic rating for transformers in a distribution network, in: ISGT 2014, 2014, pp. 1–5, http://dx.doi.org/10.1109/ISGT.2014.6816414.
[20] L. Jauregui-Rivera, X. Mao, D.J. Tylavsky, Improving reliability assessment of transformer thermal top oil model parameters estimated from measured data, IEEE Trans. Power Deliv. 24 (1) (2009) 169–176.
[21] A. Bracale, G. Carpinelli, P.D. Falco, Probabilistic risk-based management of distribution transformers by dynamic transformer rating, Int. J. Electr. Power Energy Syst. 113 (2019) 229–243, http://dx.doi.org/10.1016/j.ijepes.2019.05.048, URL http://www.sciencedirect.com/science/article/pii/S0142061519308063.
[22] A. Bracale, G. Carpinelli, P. De Falco, A predictive stress-strength model addressing the dynamic transformer rating, in: 2019 International Conference on Clean Electrical Power, ICCEP, 2019, pp. 611–616.
[23] N. Viafora, K. Morozovska, S.H.H. Kazmi, T. Laneryd, P. Hilber, J. Holbøll, Day-ahead dispatch optimization with dynamic thermal rating of transformers and overhead lines, Electr. Power Syst. Res. 171 (2019) 194–208, http://dx.doi.org/10.1016/j.epsr.2019.02.026, URL http://www.sciencedirect.com/science/article/pii/S0378779619300902.
[24] J. McCarthy, Analysis of Transformer Ratings in a Wind Farm Environment (Masters dissertation), Dublin Institute of Technology, Dublin, 2010.
[25] O.D. Ariza Rocha, K. Morozovska, T. Laneryd, O. Ivarsson, C. Ahlrot, P. Hilber, Dynamic rating assists cost-effective expansion of wind farms by utilizing the hidden capacity of transformers, Int. J. Electr. Power Energy Syst. 123 (2020) 106188, http://dx.doi.org/10.1016/j.ijepes.2020.106188, URL https://www.sciencedirect.com/science/article/pii/S0142061520302374.
[26] N. Viafora, J. Holbøll, S.H.H. Kazmi, T.H. Olesen, T.S. Sørensen, Load dispatch optimization using dynamic rating and optimal lifetime utilization of transformers, in: 2019 IEEE Milan PowerTech, 2019, pp. 1–6.
[27] S.H.H. Kazmi, J. Holbøll, T.H. Olesen, T.S. Sørensen, Dynamic thermoelectric modelling of oil-filled transformers for optimized integration of wind power in distribution networks, in: 25th International Conference on Electricity Distribution, CIRED 2019, 2019, pp. 3–6.
[28] K. Morozovska, Dynamic Rating of Power Lines and Transformers for Wind Energy Integration, in: TRITA-EECS-AVL, (no. 2018:37) KTH, Electromagnetic Engineering, Stockholm, Sweden, 2018, p. 54, QC 20180423.
[29] A. Molina Gómez, K. Morozovska, T. Laneryd, P. Hilber, Optimal sizing of the wind farm and wind farm transformer using MILP and dynamic transformer rating, Int. J. Electr. Power Energy Syst. 136 (2022) 107645, http://dx.doi.org/10.1016/j.ijepes.2021.107645, URL https://www.sciencedirect.com/science/article/pii/S0142061521008772.
[30] Y. Li, Y. Wang, Q. Chen, Optimal dispatch with transformer dynamic thermal rating in ADNs incorporating high PV penetration, IEEE Trans. Smart Grid 12 (3) (2021) 1989–1999, http://dx.doi.org/10.1109/TSG.2020.3037874.
[31] IEC, IEC 60076-2:2011 Power transformers - Part 1: General, 60076 (2), 2011.
[32] W. Szwander, The valuation and capitalization of transformer losses, J. Inst. Electr. Eng. II 92 (1945) 125–134(9). URL https://digital-library.theiet.org/content/journals/10.1049/ji-2.1945.0033.
[33] IEEE guide for loss evaluation of distribution and power transformers and reactors, IEEE Std C57.120-2017 (Revision of IEEE Std C57.120-1991), 2017, pp. 1–53, http://dx.doi.org/10.1109/IEEESTD.2017.8103991.
[34] IEEE guide for loading mineral-oil-immersed transformers and step-voltage regulators. IEEE Std C57.91-2011, IEEE Std C57.91-2011 (Revision of IEEE Std C57.91-1995), 2012, pp. 1–123, http://dx.doi.org/10.1109/IEEESTD.2012.6166928.
[35] IEC, IEC 60076-7:2017 Power transformers - Part 7: Loading guide for oil-immersed power transformers 60076 (7), 2017.
[36] N. Sönnichsen, Energy commodity price index 2035, 2021, URL https://www.statista.com/statistics/252795/weighted-price-index-of-energy/.
[37] P. Lam, The rate of return for electricity distribution networks. Discussion paper DP-26, 1988.
[38] Infographic, 2021, URL https://www.absolar.org.br/en/market/infographic/.
[39] L.F.N. Lourenço, R.M. Monaro, M.B.C. Salles, J.R. Cardoso, L. Quéval, Evaluation of the reactive power support capability and associated technical costs of photovoltaic farms operation, Energies 11 (2018) 1567.